J|A|C|S
ARTICLES
Published on Web 01/17/2007

Six-fold Oxygen-Coordinated Triplet ($S = 1$) Palladium(II) Moieties Templated by Tris(bipyridine)ruthenium(II) Ions

Fabrice Pointillart,[†] Cyrille Train,*[,†] Françoise Villain,[†,‡] Christophe Cartier dit Moulin,[†,‡] Patrick Gredin,[§] Lise-Marie Chamoreau,[†] Michel Gruselle,[†] Gabriel Aullon,[||] Santiago Alvarez,[||] and Michel Verdaguer*[,†]

Contribution from the Laboratoire de Chimie Inorganique et Matériaux Moléculaires, UMR CNRS 7071, Université Pierre et Marie Curie-Paris 6, 4 place Jussieu, Case 42, 75252 Paris Cedex 05, France, LURE, Bât. 209D, Université Paris-Sud, 91898 Orsay Cedex, France, Laboratoire de Chimie de la Matiére Condensée de Paris, UMR CNRS 7574, Université Pierre et Marie Curie-Paris 6, 4 place Jussieu, Case 176, 75252 Paris Cedex 05, France, and Department of Quimica Inorganica, Universitat Barcelona, Diagonal 647, Barcelona E-08028, Spain

Received September 21, 2006; E-mail: train@ccr.jussieu.fr; miv@ccr.jussieu.fr

Abstract: Tris(bipyridine)ruthenium(II) is used as a templating agent to insert palladium(II) into three-dimensional oxalate-based networks. The templated-assembly of $[Ru(bpy)_3][Pd_2(ox)_3]$ (**Pd2**) and $[Ru(bpy)_3][PdMn(ox)_3]$ (**PdMn**) is described. The latter compound is structurally characterized by powder X-ray diffraction and X-ray absorption spectroscopy. These techniques reveal an unusual 6-fold oxygen environment around the Pd(II) atoms with two short (2.02 Å) and four long (2.17 Å) Pd−O distances. As stated by magnetometry, this environment is associated with a triplet ground state ($S = 1$) of the palladium(II) ion: when the temperature is decreased, the $\chi_M T$ product shows a monotonous decrease from 5.54 cm^3 K mol^{-1} at 300 K, a value which is slightly lower than the one expected for independent paramagnetic Pd(II) ($S = 1$, $g = 2$) and Mn(II) ($S = {}^5/_2$, $g = 2$) ions. This thermal variation is due to antiferromagnetic exchange interactions between the two spin bearers. Nevertheless, no long-range magnetic order is detected down to 2 K. These results are confirmed by an analysis of the $[M^{II}(C_2O_4)_3]^{4-}$ (M = Ni, Pd, Pt) complex and of a $[Pd^{II}\{\mu\text{-}(C_2O_4)Mn^{II}(OH_2)_4\}_3]^{2+}$ tetranuclear model using density functional theory.

Introduction

Self-organization processes are of crucial importance in the synthesis of molecule-based materials.[1] Through a detailed analysis of the intermolecular forces between the implied moieties, the choice of the building blocks allows one to forecast the topology of the final material. To optimize these interactions, the symmetry and the size of the different moieties implied for building the final compound are key points. The use of complementary molecular elements indeed allows the best packing in the solid state.[2]

Tris(2,2′-bipyridine)metal cationic complexes have exemplified an efficient templating activity in the synthesis of three-dimensional (3D) 10-gon 3-connected (10,3) oxalate-based anionic networks. They allowed the introduction of metal ions such as Mn(II),[3−5] Co(II),[6] Ni(II), and Cu(II)[7] in such anionic networks starting from the "naked" metal ions and free ligand. When these M(II) divalent ions are mixed with oxalate in water without any template cation, linear chains of formula $[M^{II}(ox)(H_2O)_n]_\infty$ ($ox^{2-} = C_2O_4^{2-}$; $n = 0$, $^1/_3$, 1, or 2) are formed.[8] This experimental evidence underlines the key role of the tris(2,2′-bipyridine)metal cationic complexes in the formation of the 3D (10,3) networks. In these compounds, the divalent metal ions adopt a (slightly distorted) octahedral environment. The organization process obviously relies on the charge of the ionic species and, in a more subtle but decisive way, on both the D_3 symmetry and the size of the tris(bipyridine) cations. After ion pairing, the 3D (10,3) anionic network is indeed built by successive wrappings of oxalate and metal ions around the template cations.[5,7] Moreover, exploiting the configurational inertness of $[Ru(bpy)_3]^{2+}$ and $[Ru(bpy)_2(ppy)]^+$ (bpy = 2,2′-bipyridine; ppy = 2-phenylpyridine-H^+), it has been possible to control the configuration of all of the metal ions in the final

[†] Laboratoire de Chimie Inorganique et Matériaux Moléculaires, Université Pierre et Marie Curie.
[‡] Université Paris-Sud.
[§] Laboratoire de Chimie de la Matiére Condensée de Paris, Université Pierre et Marie Curie.
[||] Universitat Barcelona.

(1) Lehn, J.-M. *La Chimie Supramoléculaire, Concepts et Perspectives*; de Boeck Université: Paris, Bruxelles, 1997.
(2) Simon, J.; Bassoul, P. *Design of Molecular Materials, Supramolecular Engineering*; John Wiley & Sons: Chichester, 2000.
(3) Decurtins, S.; Schmalle, H. W.; Schneuwly, P.; Ensling, J.; Guetlich, P. *J. Am. Chem. Soc.* **1994**, *116*, 9521.
(4) Decurtins, S.; Schmalle, H. W.; Pellaux, R.; Schneuwly, P.; Hauser, A. *Inorg. Chem.* **1996**, *35*, 1451.
(5) Pointillart, F.; Train, C.; Boubekeur, K.; Gruselle, M.; Verdaguer, M. *Tetrahedron: Asymmetry* **2006**, *17*, 1937.
(6) Hernandez-Molina, M.; Lloret, F.; Ruiz-Perez, C.; Julve, M. *Inorg. Chem.* **1998**, *37*, 4131.
(7) Pointillart, F.; Train, C.; Gruselle, M.; Villain, F.; Schmalle, H. W.; Talbot, D.; Gredin, P.; Decurtins, S.; Verdaguer, M. *Chem. Mater.* **2004**, *16*, 832.
(8) Verdaguer, M.; Julve, M.; Michalowicz, A.; Kahn, O. *Inorg. Chem.* **1983**, *22*, 2624.

10.1021/ja066817v CCC: $37.00

Table 2. Literature Data for Six-Coordinated Palladium(II) Together with the Octahedral Shape Measures $S(O_h)$[a]

compd	structure	Pd–X /Å	magnetism	$S(O_h)$	ref
PdF_2	OC-6	2.16	triplet	1.20	12
	OC-6	2.16	n.a.	0.78	16
HP-PdF_2	OC-6		triplet	1.48	14
	OC-6		n.a.	1.19	13
$KPdF_3$	OC-6	2.12	n.a.	0.00	16
$RbPdF_3$	OC-6	2.15	n.a.	0.00	16
$CsPd_2F_5$	OC-6	2.14	triplet	0.35	17
$LiPdGaF_6$	OC-6	2.19	n.a.	0.00	18
$RbPdAlF_6$	OC-6	2.16	n.a.	1.16	18
$PdAu_2F_8$	OC-6	2.17	n.a.	0.42	19
$PdZrF_6$	OC-6	2.10	n.a.	0.00	15
$PdAs_2O_6$	OC-6	2.24	triplet	0.15	21
HT-Ca_2PdWO_6	OC-6	2.17	n.a.	0.00	20
LT-Ca_2PdWO_6	OC-6	2.17	n.a.	0.46	20
		2.08−2.25	n.a.	0.43	
PdO	4+2	2.1, 2.7	n.a.	1.40	23
thin film PdO	OC-6	2.82	n.a.	0.00	51
PdN_2S_4	4+2	2.2, 3.0	singlet	4.14	25
$PdO_2P_2O_2$	4+2	2.2, 2.6	singlet	3.47	52
PdS_4Cl_2	4+2	2.3, 3.18	singlet	6.57	26
$PdAs_4I_2$	4+2	2.4, 3.4	n.a.	3.27	53

[a] HP, HT, and LT stand for high pressure, high temperature, and low temperature, respectively. OC-6 stands for octahedral (six nearly equivalent Pd−ligand bond distances), and 4+2 indicates a tetragonally distorted geometry with four short and two long distances. n.a. stands for not available.

material starting from resolved template cations for both powdered samples and single crystals.[5,9] We have shown that these supramolecular constraints can create original new surroundings around metal ions such as Cu(II) and Ni(II),[7] and we intend to extend this work to second or third series divalent transition metal ions, palladium(II) and platinum(II).

These two ions usually adopt a square-planar symmetry that allows an important gain of electronic energy for this d^8 cation as compared to an octahedral coordination mode.[10] These ions are indeed used in supramolecular chemistry as square-planar coding units.[11] For palladium(II), two noticeable exceptions appear in solid-state chemistry. The first one is fluorine-based palladium(II) compounds[12−19] (see Table 2). For example, $Pd^{II}F_2$ crystallizes in a rutile type structure where the Pd(II) is surrounded by 4 fluorides at 2.155 Å and 2 fluorides at 2.171 Å.[12] The second exception is two complex oxides, Ca_2PdWO_6[20] and $PdAs_2O_6$[21] (see Table 2). In the latter compound, Pd(II) is surrounded by six oxygen atoms located at 2.24 Å.[21] On the contrary, in pristine PdO, the divalent metal ion is in a square-planar environment.[22,23] Coordination chemists have employed a wide variety of sulfur-containing multidentate and/or macrocyclic ligands to stabilize six-coordinated complexes of palladium(II) and platinum(II) relying on both the softness of the sulfur atoms and the supramolecular influence of the ligand.[24−26] In the structures described for palladium(II), the metal ion is surrounded by four atoms in a square-planar arrangement close to the metal ions, for example, Pd−N in the 2.06−2.10 Å range, Pd−S and Pd−Cl in the 2.26−2.36 Å range, and by two axial sulfur atoms located at long distances varying between 2.96 and 3.27 Å, only slightly shorter than the sum of the Van der Walls radii of the two atoms (3.43 Å). No example is reported for platinum(II) in the Cambridge Structural Database (CSD).[27]

Obtaining these ions in a 6-fold environment within a 3D (10,3) anionic network would allow one to evaluate the templating activity of tris(2,2′-bipyridine)metal complexes. It indeed requires imposing strong constraints to these ions at the supramolecular level to overcome the loss of electronic energy at the molecular level associated with this coordination mode.

We report our synthetic efforts to use the strong templating activity of $[Ru(bpy)_3]^{2+}$ to obtain a 6-fold environment to palladium(II) and platinum(II). The syntheses of $[Ru^{II}(bpy)_3][Pd^{II}_2(ox)_3]$ noted **Pd2** and $[Ru^{II}(bpy)_3][Pd^{II}Mn^{II}(ox)_3]$ noted **PdMn** are described. For **PdMn**, the combined analysis of powder X-ray diffraction (XRD) and X-ray absorption spectroscopy (SAX) is used to give a complete view of the structural organization of the polycrystalline material. The structural and magnetic properties of this compound are then presented and discussed in the light shed by a computational study based on the density functional theory (DFT).

(9) Andres, R.; Brissard, M.; Gruselle, M.; Train, C.; Vaissermann, J.; Malezieux, B.; Jamet, J.-P.; Verdaguer, M. *Inorg. Chem.* **2001**, *40*, 4633.
(10) Jean, Y. *Les Orbitales Moléculaires dans les Complexes*; les Editions de l'Ecole Polytechnique: Palaiseau, 2003. Jean, Y. *Molecular Orbitals of Transition Metal Complexes*; Oxford University Press: Oxford, 2005.
(11) He, W.; Liu, F.; Duan, C.; Guo, Z.; Zhou, S.; Liu, Y.; Zhu, L. *Inorg. Chem.* **2001**, *40*, 7065.
(12) Bartlett, N.; Maitland, R. *Acta Crystallogr.* **1958**, *11*, 747.
(13) Tressaud, A.; Soubeyroux, J. L.; Touhara, H.; Demazeau, G.; Langlais, F. *Mater. Res. Bull.* **1981**, *16*, 207.
(14) Mueller, B. G. *J. Fluorine Chem.* **1982**, *20*, 291.
(15) Bachmann, B.; Mueller, B. G. *Z. Anorg. Allg. Chem.* **1993**, *619*, 189.
(16) Bachmann, B.; Mueller, B. G. *Z. Anorg. Allg. Chem.* **1993**, *619*, 387.
(17) Ruchaud, N.; Grannec, J.; Tressaud, A.; Ferey, G. *Z. Anorg. Allg. Chem.* **1995**, *621*, 1958.
(18) Mueller, M.; Mueller, B. G. *Z. Anorg. Allg. Chem.* **1995**, *621*, 1385.
(19) Bialowons, H.; Mueller, B. G. *Z. Anorg. Allg. Chem.* **1997**, *623*, 434.
(20) Fu, Z.-M.; Li, W.-X. *Sci. China* **1996**, *39*, 981.
(21) Orosel, D.; Jansen, M. *Z. Anorg. Allg. Chem.* **2006**, *632*, 1131.
(22) Wells, A. F. *Structural Inorganic Chemistry*, 5th ed.; Clarendon Press: Oxford, 1984.
(23) Christy, A. G.; Clark, S. M. *Phys. Rev. B* **1995**, *52*, 9259.
(24) Wieghardt, K.; Küppers, H.-J.; Raabe, E.; Krüger, C. *Angew. Chem., Int. Ed. Engl.* **1986**, *25*, 1101. Blake, A. J.; Gould, R. O.; Lavery, A. J.; Schröder, M. *Angew. Chem., Int. Ed. Engl.* **1987**, *25*, 274. Blake, A. J.; Holder, A. J.; Hyde, T. I.; Roberts, Y. V.; Lavery, A. J.; Schröder, M. *J. Organomet. Chem.* **1987**, *323*, 261. Blake, A. J.; Reid, G.; Schröder, M. *J. Chem. Soc., Dalton Trans.* **1990**, 3363. Grant, G. J.; Sanders, K. A.; Setzer, W. N.; VanDerveer, D. G. *Inorg. Chem.* **1991**, *30*, 4053. Chandrasekhar, S.; McAuley, A. *Inorg. Chem.* **1992**, *31*, 2663. Blake, A. J.; Crofts, R. D.; de Groot, B.; Schröder, M. *J. Chem. Soc., Dalton Trans.* **1993**, 485.
(25) Reid, G.; Blake, A. J.; Hyde, T. I.; Schröder, M. *J. Chem. Soc., Chem. Commun.* **1988**, 1397.
(26) Takeda, N.; Shimizu, D.; Tokitoh, N. *Inorg. Chem.* **2005**, *44*, 8561.
(27) Allen, F. *Acta Crystallogr., Sect. B: Struct. Sci.* **2002**, *58*, 380.

Experimental Section

Materials. We have followed experimental procedures described in the literature to prepare $[Ru(bpy)_3]X_2$ (X = Cl, I)[28] and the enantiomerically enriched (Δ)- and (Λ)-isomers of $[Ru(bpy)_3]^{2+}$.[29] The other reagents are commercially available and were used as purchased.

Synthesis. Pd2. An aqueous solution (1 cm^3) containing 29.4 mg of Na_2PdCl_4 ($M = 294.4$ g mol^{-1}, $n = 0.1$ mmol) was added dropwise to an aqueous solution (2 cm^3) containing 37.4 mg of $[Ru(bpy)_3]Cl_2 \cdot 6H_2O$ ($M = 748$ g mol^{-1}, $n = 5 \times 10^{-2}$ mmol) and 27.6 mg of $K_2C_2O_4 \cdot H_2O$ ($M = 184$ g mol^{-1}, $n = 0.15$ mmol). After 60 min, the precipitate was filtered off, washed with water, and air-dried to yield 44.9 mg (89.8%) of an orange solid characterized as $[Ru(bpy)_3][Pd_2(ox)_3]$. Anal. Calcd for $C_{36}H_{24}N_6O_{12}Pd_2Ru$: C, 41.31; H, 2.29; N, 8.03; Pd, 20.35; Ru, 9.66. Found: C, 40.89; H, 3.28; N, 8.38; Pd, 15.15; Ru, 8.83.[31]

IR (KBr pellet)/cm^{-1}: 3102, 3070 (ν(C−H)), 1698, 1674 (ν_{AS}(C═O)), 1463, 1444, 1421 (ν(C−C)), 1400, 1379 (ν_S(C═O)), 821 (δ(C═O)), 771 (δ(C−H)).

PdMn. An aqueous solution (1 cm^3) containing 14.7 mg of Na_2PdCl_4 ($M = 294.4$ g mol^{-1}, $n = 0.05$ mmol) and 9.9 mg of $MnCl_2 \cdot 4H_2O$ ($M = 198$ g mol^{-1}, $n = 5 \times 10^{-2}$ mmol) was added dropwise to an aqueous solution (2 cm^3) containing 37.4 mg of $[Ru(bpy)_3]Cl_2 \cdot 6H_2O$ ($M = 748$ g mol^{-1}, $n = 5 \times 10^{-2}$ mmol) and 27.6 mg of $K_2C_2O_4 \cdot H_2O$ ($M = 184$ g mol^{-1}, $n = 0.15$ mmol). After 60 min, the precipitate was filtered off, washed with water, and air-dried to yield 41.7 mg (83.4%) of an orange solid characterized as $[Ru(bpy)_3][PdMn(ox)_3]$. Anal. Calcd for $C_{36}H_{24}N_6O_{12}PdMnRu$: C, 43.45; H, 2.41; N, 8.45; Mn, 5.52; Pd, 10.69; Ru, 10.16. Found: C, 43.47; H, 2.62; N, 8.45; Mn, 4.16; Pd, 7.66; Ru, 9.50.[31]

IR (KBr pellet)/cm^{-1}: 3101, 3073 (ν(C−H)), 1699, 1670, 1630, 1607 (ν_{AS}(C═O)), 1456, 1444, 1421 (ν(C−C)), 1360, 1315, 1309 (ν_S(C═O)), 797 (δ(C═O)), 777 (δ(C−H)).

Single-Crystal Growth of $[Ru(bpy)_3][Pd_2Cl_6] \cdot {}^1/_2H_2O$. A typical crystallization experiment consisted of the formation of a silica gel by mixing $Si(OCH_3)_4$ (2 cm^3), CH_3OH (2 cm^3), and a 2 cm^3 aqueous solution containing 16.5 mg of potassium oxalate (0.090 mmol) and 22.4 mg of $[Ru(bpy)_3]Cl_2 \cdot 6H_2O$ (3.0×10^{-2} mmol). The resulting orange solution was placed in a test tube. A gel formed overnight, and an aqueous solution (3 cm^3) containing 17.6 mg of Na_2PdCl_4 (0.06 mmol) was added upon the gel. After 1 week, parallelepipedic-shaped dark red crystals formed.

Single-Crystal Growth of $[Ru(bpy)_3]_2[Pd(ox)_2][PdCl_4] \cdot 11H_2O$. The red single crystals are obtained by slowly evaporating the filtrate of the reaction leading to powdered **Pd2** samples.

Experimental Techniques. Elemental analyses were completed at the SIARE-UPMC, Paris and at the Service Central d'Analyse of the Centre National de la Recherche Scientifique (CNRS) in Vernaison, France.

Single-Crystal Structure Determination. A single crystal of each compound was selected, mounted onto a glass fiber, and transferred in a cold nitrogen gas stream. Intensity data were collected with a Bruker-Nonius Kappa-CCD with graphite-monochromated Mo Kα radiation. Unit-cell parameters determination, data collection strategy, and integration were carried out with the Nonius EVAL-14 suite of programs.[30] Crystal parameters and collection details are summarized in Table 1.

Table 1. Crystal Data and Structure Refinement Parameters for $[Ru^{II}(bpy)_3][Pd^{II}{}_2Cl_6] \cdot {}^1/_2H_2O$ and $[Ru^{II}(bpy)_3]_2[Pd^{II}(ox)_2][Pd^{II}Cl_4] \cdot 11H_2O$

	$[Ru^{II}(bpy)_3][Pd^{II}{}_2Cl_6] \cdot {}^1/_2H_2O$	$[Ru^{II}(bpy)_3]_2[Pd^{II}(ox)_2][Pd^{II}Cl_4] \cdot 11H_2O$
formula	$C_{60}H_{50}Cl_{12}N_{12}OPd_4Ru_2$	$C_{64}H_{70}Cl_4N_{12}O_{19}Pd_2Ru_2$
cryst syst	triclinic	monoclinic
space group	*P*-1	$P2_1$
a (Å)	16.302(3)	12.4366(17)
b (Å)	16.465(3)	25.409(3)
c (Å)	16.551(2)	12.862(3)
α (deg)	101.751(11)	90.00
β (deg)	111.493(9)	113.313(12)
γ (deg)	113.567(11)	90.00
V (Å^3)	3454(11)	3733(1)
Z	2	2
D_{calcd} (g cm^{-3})	1.93	1.66
M (g mol^{-1})	2008.26	1868.08
μ (cm^{-1})	19.59	10.9
size (mm)	0.15 × 0.13 × 0.04	0.22 × 0.38 × 0.40
color	dark red	red
shape	parallelepiped	block
diffractometer	Nonius Kappa-CCD	Nonius Kappa-CCD
temperature (K)	250	180
radiation type	Mo Kα	Mo Kα
wavelength (Å)	0.710730	0.710730
scan type	Φ scan (ΔΦ = 2°)	Φ scan (ΔΦ = 2°)
reflns measd	82 373	25 501
indep reflns	23 610	15 034
R_{int}	0.078	0.080
θ min, max	1, 32.00	1, 27.00
h_{min}, h_{max}	−24, 24	−15, 15
k_{min}, k_{max}	−24, 24	−32, 32
l_{min}, l_{max}	−24, 24	−15, 16
refinement	on F^2	on *F*
$R(F)$	0.0432	0.0578
$R_w(F^2)$ all data	0.0895	0.0645
$\Delta\rho$ min (ē/Å^3)	−1.02	−2.84
$\Delta\rho$ max (ē/Å^3)	0.76	2.74
reflns used	23 610	11 153
$\sigma(I)$ limit	2.00	3.00
no. of variables	820	815
GOF	0.95	1.077

The structure of $[Ru(bpy)_3][Pd_2Cl_6] \cdot {}^1/_2[H_2O]$ was solved by direct methods using the SHELXS-97 program and refined anisotropically by full-matrix least-squares methods using the SHELXL-97 software package.[31] The structure of $[Ru(bpy)_3]_2[Pd(ox)_2][PdCl_4] \cdot 11H_2O$ was solved by direct methods using the SIR92 program[32] and refined by full matrix least-squares on *F* by using the programs of the PC version of CRYSTALS.[33] Crystallographic data (excluding structure factors) for the structures reported in this paper have been deposited at the Cambridge Crystallographic Data Centre with CCDC numbers 621724 and 621725.

Powder X-ray Diffraction. The powder diffraction patterns were collected at room temperature on a Philips PW-1050 goniometer using the Bragg−Brentano configuration and Mn-filtered Fe Kα radiation. The X-ray powder patterns were first analyzed by the EVA program.[34] The cell parameters were refined using the UFIT program.[35] Although the diffraction peaks are thin, their profile prevents the Rietveld refinement from proceeding.

X-ray Absorption Spectroscopy (XAS). XAS experiments were performed on the XAS 4 beam line at the French synchrotron facility DCI at LURE (Orsay). At K-edges, the samples were ground and homogeneously dispersed in cellulose pellets, while at Pd $L_{2,3}$-edges, they were prepared as thin self-supporting wafers. Spectra were recorded

(28) Broomhead, J. A.; Young, C. G. *Inorg. Synth.* **1982**, *21*, 127.
(29) Dwyer, F. P.; Gyarfas, E. C. *J. Proc. R. Soc. N. S. W.* **1949**, *83*, 174.
(30) Duisenberg, A. J. M.; Kroon-Batenburg, L. M. J.; Schreurs, A. M. M. *J. Appl. Crystallogr.* **2003**, *36*, 220.
(31) In **Pd2**, the ratio Pd/Ru is 2/1.23 (±0.2). In **PdMn**, the ratios Mn/Pd/Ru are 1/0.95/1.24 (±0.20). These results are in line with those obtained on comparable 3D oxalate-based compounds. The ratio of the metal(s) inserted in the anionic network to the ruthenium of the template cation is slightly the same for **PdMn** and **Pd2**. For **PdMn**, the Mn/Pd ratio is coherent with the nominal value of 1/1. Moreover, this ratio was confirmed by the absorbance of the sample measured at Pd and Mn K-edges. Finally, it should be noted that a Mn/Pd ratio significantly different from 1/1 would spoil the observed agreement between experimental and calculated percentages for C, H, and N, because of the important molar mass difference between palladium and manganese.

(32) Sheldrick, G. M. *SHELXL97*; University of Göttingen: Germany, 1997.
(33) Altomare, A.; Cascarano, G.; Giacovazzo, C.; Guagliardi, A. *J. Appl. Crystallogr.* **1993**, *26*, 343.
(34) Betteridge, P. W.; Carruthers, J. R.; Cooper, R. I.; Prout, K.; Watkin, D. J. *J. Appl. Crystallogr.* **2003**, *36*, 1487.
(35) Caussin, P.; Nusinovici, J.; Beard, D. W. *Adv. X-ray Anal.* **1988**, *31*, 423. Caussin, P.; Nusinovici, J.; Beard, D. W. *Adv. X-ray Anal.* **1989**, *32*, 531.

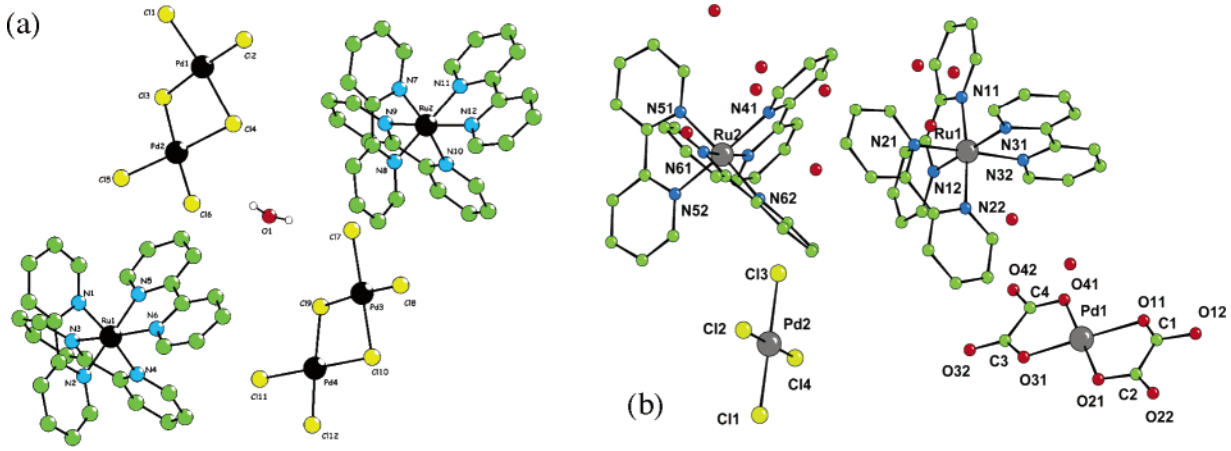

Figure 1. Crystal structures of $[Ru^{II}(bpy)_3][Pd^{II}_2Cl_6]\cdot{}^1/_2H_2O$ (a) and $[Ru^{II}(bpy)_3][Pd^{II}Cl_4][Pd^{II}(ox)_2]\cdot 11H_2O$ (b).

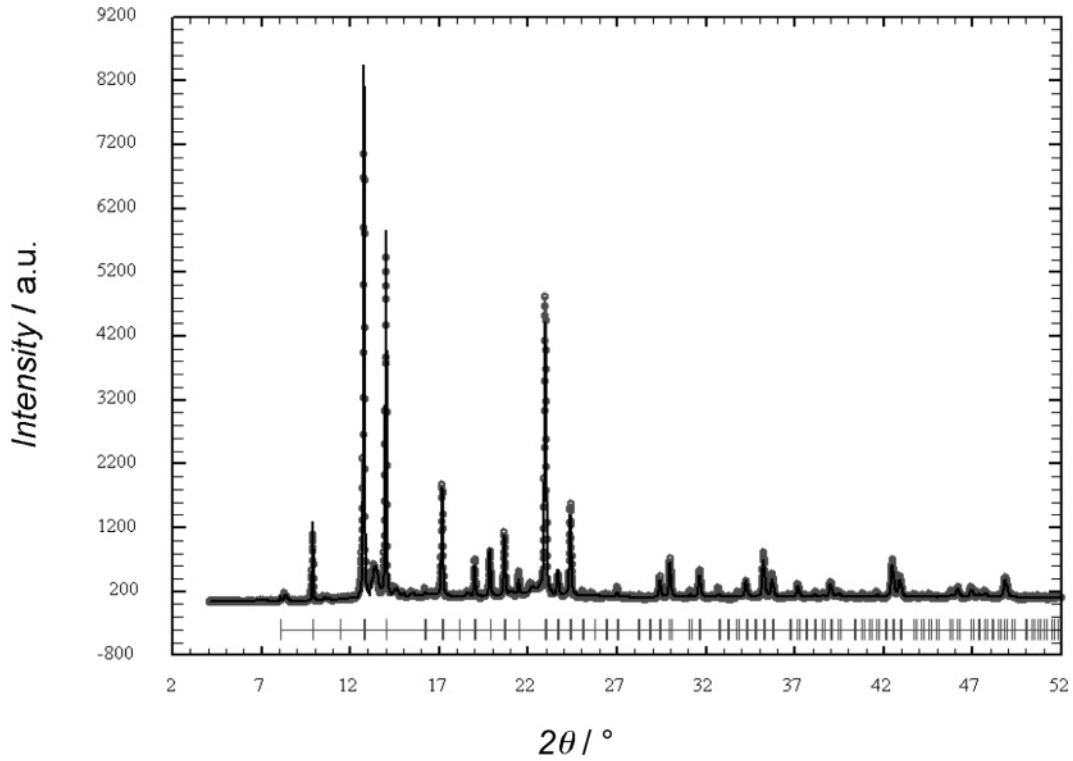

Figure 2. Observed (circle) and calculated (full curve) X-ray powder diffraction pattern profile of **PdMn** at room temperature. The short vertical lines below the profile curves mark all possible Bragg reflections.

in transmission mode using the double monochromators. At the Pd K-edge, the Mn K-edge, and the Pd $L_{2,3}$-edges, the experiment was calibrated with a Pd, a Mn, and a Ti metallic foil at 24 350, 6540, and 4965 eV, respectively, for the first inflection point of the absorption spectrum. The background of the near-edge spectra at the Pd K-edge was subtracted by fitting the pre-edge with a linear function. The adsorption spectra were normalized at the middle of the first EXAFS oscillation. At the Pd $L_{2,3}$-edges, the background was subtracted by fitting the pre-edge with a Victoreen function, and the adsorption spectra were normalized at 3200 eV. The EXAFS treatment was performed with the "EXAFS pour le MAC" code.[36] The simulations were realized on the inverse Fourier transforms of the first shell of neighbors in the framework of single scattering scheme with the Round Midnight program.[37] They were achieved using the amplitude ($|f_i(k,R_i)|$) and phase ($|\phi_i(k,R_i)|$ functions of Pd−O pairs and Mn−O pairs calculated with the FEFF7 code[38] from crystallographic data of $[Pd^{II}(acac)_2]$ and MnO, respectively. Details on this technique are proposed as Supporting Information.

Magnetic Measurement. The magnetization of powdered samples was measured between 2 and 300 K on a Quantum Design MPMS5 squid magnetometer. The susceptibility was measured in a 0.1 T external field and corrected for the diamagnetism of the container and the compound itself.

Computational Details for the DFT Calculation. Density functional unrestricted calculations were carried out with the Gaussian 98 package,[39] using the hybrid method known as B3LYP that is character-

(36) Evain, M. I.M.N.: Nantes, France, 1992.

(37) Michalowicz, A. *EXAFS pour le MAC*; Société Française de Chimie: Paris, France, 1991.
(38) James, F.; Roos, M. *Round Midnight*; CERN Computing Center, Program Library, CERNID Internal Report 75/20, 1976.
(39) Rehr, J. J.; Mustre de Leon, J.; Zabinsky, S. I.; Albers, R. C. *J. Am. Chem. Soc.* **1991**, *113*, 5135.

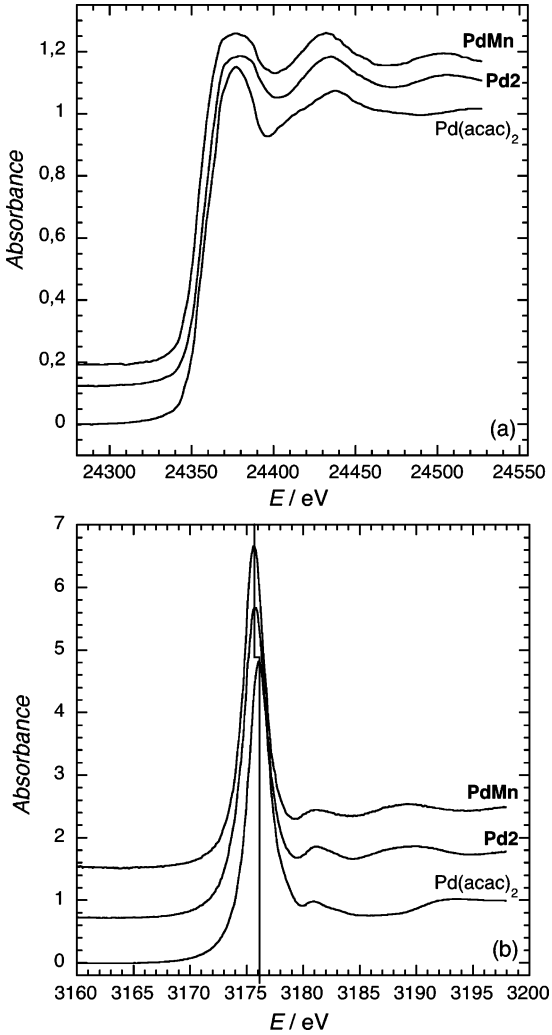

Figure 3. Near-edge structures spectra (XANES) at palladium K-edge (a) and L_3-edge (b) for **PdMn**, **Pd2**, and $[Pd^{II}(acac)_2]$.

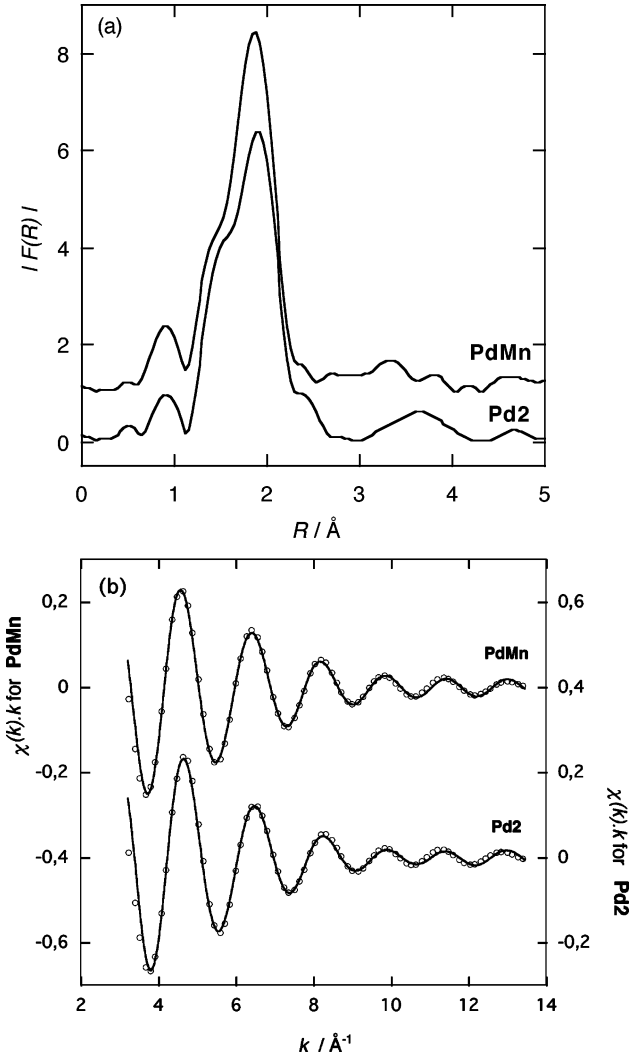

Figure 4. Modulus of the Fourier transforms of the EXAFS signals of **PdMn** and **Pd2**. (a) Experimental EXAFS signal at Pd K-edge of **PdMn** and **Pd2** arising from the first shell (○) as compared to the simulation for the optimized geometry (see text) (b).

ized by the Becke three parameters hybrid exchange functional[40] and the Lee−Yang−Parr correlation functional.[41] Relativistic effective core potentials (RECP) from the Stuttgart−Dresden group were used to represent the innermost electrons of the Pd[42] and Mn[43] atoms, together with their associated valence basis set of double-ζ quality. The basis set for light elements (C, O, and H) was also double-ζ for the valence orbitals with a polarization function in all atoms.[44] These results have been tested by adding an extra diffuse function for C and O in $[Pd(ox)_3]^{4-}$ species (exponents 0.0438 and 0.0845, respectively, as included in the 6-31+G* family).[45] The electronic configurations have been confirmed through Mulliken and natural population analysis.

Results and Discussion

Synthesis. Compounds **Pd2** and **PdMn** are obtained as bright orange microcrystalline powders by mixing a solution containing $[Ru(bpy)_3]^{2+}$, $2Cl^-$ and $2K^+$, $C_2O_4^{2-}$ to a solution containing $2Na^+$, $[PdCl_4]^{2-}$ and, for **PdMn**, Mn^{2+}, $2NO_3^-$. This operating mode contrasts with those previously described:[3,6,7] mixing $[Ru(bpy)_3]^{2+}$ with $[PdCl_4]^{2-}$ indeed leads to the formation of $[Ru(bpy)_3][Pd_2Cl_6]$. Mixing $[PdCl_4]^{2-}$ with ox^{2-} before introducing $[Ru(bpy)_3]^{2+}$ leads to the formation of $K_2[Pd(ox)_2]\cdot 4H_2O$ where Pd(II) is in a square-planar environment, surrounded by the four oxygen atoms of the two oxalate ligands. No single crystals of **Pd2** and **PdMn** could be obtained. Our attempts to obtain single crystals of **Pd2** using the gel technique led to the slow formation of single crystals of $[Ru^{II}(bpy)_3][Pd^{II}_2Cl_6]\cdot {}^1/_2H_2O$ (Figure 1a). Using the slow evaporation technique, we end up with single crystals of $[Ru^{II}(bpy)_3]_2[Pd^{II}Cl_4][Pd^{II}(ox)_2]\cdot 11H_2O$ (Figure 1b). In both structures, the Pd(II) ions adopt the common square-planar geometry. In the former compound, the terminal Pd−Cl distances are in the 2.25−2.29 Å range and the bridging ones in the 2.29−2.36 Å range. In the latter compound, the Pd−Cl distances are in the 2.29−2.31 Å range and the Pd−O ones in the 2.00−2.13 Å range. This influence of the reaction time on the final compound is a strong indication that the templated-assembly of **Pd2** and **PdMn** is based on a kinetic control of the reaction. The operating mode could not be extended to analogous platinum(II) materials. This observation sets an upper limit of the templating activity of $[Ru^{II}(bpy)_3]^{2+}$.

(40) Frisch, M. J.; et al. *Gaussian 98*, revision A.11; Gaussian, Inc.: Pittsburgh, PA, 2001.
(41) Becke, A. D. *J. Chem. Phys*. **1993**, *98*, 5648. Becke, A. D. *J. Phys. Chem.* **1993**, *98*, 5648.
(42) Lee, C.; Yang, W.; Parr, R. G. *Phys. Rev. B* **1988**, *37*, 785.
(43) Andrae, D.; Haeussermann, U.; Dolg, M.; Stoll, H.; Preuss, H. *Theor. Chim. Acta* **1990**, *77*, 123.
(44) Dolg, M.; Wedig, U.; Stoll, H.; Preuss, H. *J. Chem. Phys.* **1987**, *86*, 2123.
(45) Schäfer, A.; Horn, H.; Ahlrichs, R. *J. Chem. Phys.* **1992**, *97*, 2571.

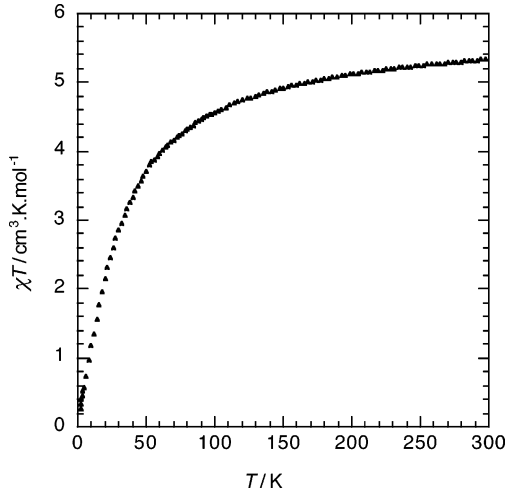

Figure 5. Thermal variation of the $\chi_M T$ product measured in a 0.1 T applied field for **PdMn**.

Because single crystals are lacking, we combined several structural techniques to obtain complementary information on the long-range and short-range structural order around the palladium and manganese atoms.

Structural Analysis. The crystallinity is much higher for **PdMn** than for **Pd2**. We thus focus our analysis on **PdMn**. The XRD pattern of **PdMn** is shown in Figure 2. The profile matching indicates that **PdMn** is isomorphous to $[Ru^{II}(bpy)_2ppy][Mn^{II}Cr^{III}(ox)_3]$.[9] **PdMn** crystallizes in the cubic chiral space group $P2_13$ with $a = 15.4834(3)$ Å. The most striking consequence of the isomorphism of **PdMn** and $[Ru^{II}(bpy)_2ppy][Mn^{II}Cr^{III}(ox)_3]$ is that, in **PdMn**, the palladium(II) is surrounded by six oxygen atoms of three bidentate oxalate ligands. According to the symmetry operations of this space group, the coordination polyhedron around Pd(II) is indeed a (trigonally distorted) octahedron.

Because XRD is sensitive to long-range order, it averages the environment of a large amount of metal ions. As demonstrated in copper(II)-containing material,[7,46] XRD may not describe properly the local environment around the metal ion in the case of orientational disorder.[47] To get a local view of this rare environment of the palladium(II), X-ray absorption spectroscopy (XAS) appears as a well-adapted technique to compare the signals arising from **PdMn** and **Pd2**.

The XAS signal was first measured at the Pd K-edge (transitions from 1s level). Figure 3a shows the near-edge structures (XANES) spectra of **PdMn** and **Pd2** together with the spectra of a reference compound, $[Pd^{II}(acac)_2]$ (acac = acetylacetonate). In $[Pd^{II}(acac)_2]$, the Pd(II) ion adopts a square-planar geometry (Pd−O distance of 1.96 Å).[48] When considering the first coordination sphere, this complex is relevant of the D_{4h} point symmetry group. The similarity of **PdMn** and **Pd2** edge structures (Figure 3a) shows that the electronic structure and the local symmetry of the Pd ions are the same in both compounds. They are different from the edge structure of $[Pd^{II}(acac)_2]$: the first maximum is more rounded and the oscillating region at high energy totally different. This indicates that the first coordination spheres of the Pd ion in **PdMn** and **Pd2** are similar and significantly modified as compared to the square-planar geometry in $[Pd^{II}(acac)_2]$. To confirm the information obtained at Pd K-edge, the XAS signal was measured at the Pd $L_{2,3}$-edges. It then corresponds to $2p^64d^8 \rightarrow 2p^54d^9$ transitions. The resolution is much better at L-edges because the core hole width is weaker.[49] At L_3-edge (Figure 3b), the maximum absorption peak energy for $[Pd^{II}(acac)_2]$ is at 3176.2 eV. For **PdMn** and **Pd2**, we observe a slight but significant downward energy shift of the peak (3175.7 eV). The same energy shift is observed at the L_2-edge (not presented). As observed at the K-edge, the spectra of **PdMn** and **Pd2** are quite similar and noticeably different from those of the square-planar $[Pd^{II}(acac)_2]$. The energy position of the maximum confirms the +II oxidation number of the palladium ion in **PdMn** and **Pd2**. A +IV oxidation number would indeed lead to a 2 eV upward shift because of a stabilization of the 2p core orbitals as compared to the 4d ones (screening effect).[50] The slight downward energy shift of the energy at the maximum of absorption in **PdMn** and **Pd2** as compared to $[Pd^{II}(acac)_2]$ corresponds to the lengthening of the Pd−O mean distance (see EXAFS analysis below) as compared to the Pd−O distance in the square-planar complex. The lengthening of the Pd−O bonds actually leads to a slight decrease of the antibonding 4d orbitals energy and hence to a downward energy shift of the absorption maximum.

To go beyond this qualitative description, we performed the quantitative analysis of the EXAFS signal collected at the Pd K-edge to determine the number of oxygen atoms around the palladium and the corresponding Pd−O distances (Figure 4). The pseudo-radial distribution functions given by the Fourier transforms of the EXAFS signals of **PdMn** and **Pd2** are shown on Figure 4a. In both compounds, the Fourier transforms exhibit one main peak with a marked shoulder at low distances. This feature is characteristic of the existence of two close Pd−O distances, the longer one corresponding to a larger number of oxygen atoms. The existence of two close distances is confirmed by the beat observed between 10 and 11 $Å^{-1}$ in the inverse Fourier transform of this first peak (Figure 4b). For both **PdMn** and **Pd2**, the fit of the whole inverse Fourier transforms confirms these conclusions: an excellent agreement with the two experimental curves is obtained with 2 oxygen atoms situated at 2.02 Å and 4 oxygen atoms situated at 2.17 Å (Figure 4b). For **PdMn**, the EXAFS signal was collected at the Mn K-edge as well. The pseudo-radial distribution function shows three main peaks. The inverse Fourier transform of the first one corresponds to the Mn−O distances. It is perfectly reproduced assuming 6 oxygen atoms located at 2.16 Å. This distance is the same as those observed in $[Ni^{II}(bpy)_3][Mn^{II}_2(ox)_3]$ and $[Ru^{II}(bpy)_3][Mn^{II}_2(ox)_3]$ by single-crystal X-ray diffraction.[3,5] The EXAFS analysis thus confirms in a quantitative way the 6-fold coordination mode of palladium(II) in **PdMn**. The 6-fold environment found for Pd(II) in **Pd2** indicates that $[Ru^{II}(bpy)_3]^{2+}$ plays his templating role at a local stage, but the better crystallinity of **PdMn** as compared to **Pd2** underlines the

(46) Clark, S. M.; Chandrasekar, J.; Spitznagel, G.; Schleyer, P. v. R. *J. Comput. Chem.* **1983**, *4*, 294.
(47) Villain, F.; Verdaguer, M.; Dromzee, Y. *J. Phys. IV* **1997**, *7*, 659.
(48) Michalowicz, A.; Verdaguer, M.; Mathey, Y.; Clément, R. In *Synchrotron Radiation in Chemistry and Biology, Topics in Current Chemistry*; Mandelkow, E., Ed.; Springer-Verlag: Berlin, 1988; Vol. 145, p 107.
(49) Knyazeva, A. N.; Shugam, E. A.; Shkolnikova, L. M. *Zh. Strukt. Khim.* **1970**, *11*, 938.
(50) Krause, M. O.; Oliver, J. H. *J. Phys. Chem. Ref. Data* **1979**, *8*, 32.
(51) Nemanova, V. I.; Kondratenko, A. V.; Ruzankin, S. F.; Bausk, N. V.; Zhidomirov, G. M.; Mazalov, L. N. *Chem. Phys.* **1987**, 116, 61. Sugiura, C.; Muramatsu, S. *J. Chem. Phys.* **1985**, *82*, 2191.
(52) Kumar, J.; Saxena, R. *J. Less-Common Met.* **1989**, *147*, 59.
(53) Sun, J.-S.; Uzelmeier, C. E.; Ward, D. L.; Dunbar, K. R. *Polyhedron* **1998**, *17*, 2049.

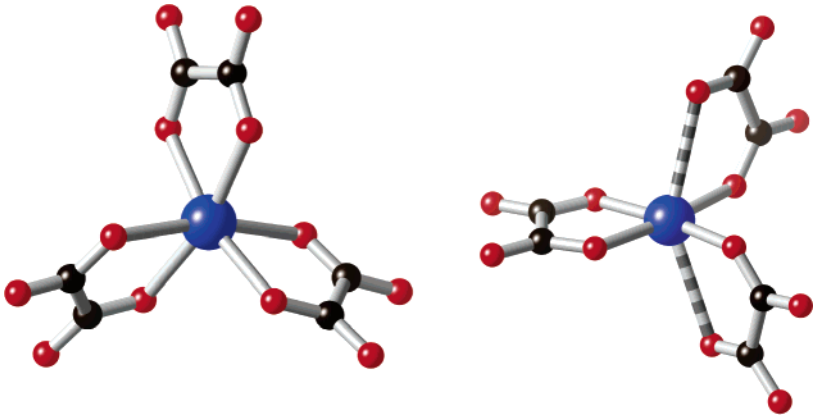

Figure 6. Optimized structure of the $[Pd^{II}(ox)_3]^{4-}$ anion in its triplet (left) and singlet (right) states.

structural role of Mn(II) to ensure a better long-range order of the anionic network.

An important consequence of the 6-fold environment of Pd(II) is the possibility for this d^8 cation to have two unpaired electrons and hence a triplet (T) ground state (GS) instead of the singlet (S) GS observed in the square-planar geometry.

Magnetic Properties. We have performed the magnetic measurement on the compound structurally characterized by both XRD and SAX, **PdMn**. The $\chi_M T$ curve shows a monotonic decrease from 5.34 cm^3 K mol^{-1} at 300 K when the temperature is decreased (Figure 5). No long-range magnetic order was detected down to 2 K. The $\chi_M T$ value at 300 K is slightly lower at 5.54 cm^3 K mol^{-1} expected for independent paramagnetic Pd(II) ($S = 1$, $g = 2$) and Mn(II) ($S = {}^5/_2$, $g = 2$) ions. The thermal evolution of $\chi_M T$ is characteristic of an antiferromagnetic (AF) coupling between the metal ions justifying the low value of $\chi_M T$ at ambient temperature. The low value of $\chi_M T$ at 2 K is attributed to the disorder of the two metal ions on the two crystallographic sites of the anionic network: the presence of antiferromagnetically coupled Mn−Mn and Pd−Pd neighbors prevents the observation of the ferrimagnetic behavior expected for a perfectly ordered array of Pd−Mn pairs. The magnetic data are a clear demonstration of the triplet nature of Pd(II).

Theoretical Analysis. Because Pd(II) in a 6-fold environment with a triplet ground state remains an exceptional situation, it is important to have a theoretical assessment of such a situation. We have carried out geometry optimizations for the two spin states of an isolated $[Pd^{II}(ox)_3]^{4-}$ anion using DFT methods with the hybrid functional B3LYP. A pseudo-octahedral structure of D_3 symmetry with six identical Pd−O distances (2.311 Å) corresponds to a triplet ground state, whereas the singlet state yields a tetragonal structure with four short (2.101 Å) and two long (2.904 Å) distances (Figure 6). Both structures have been characterized as stationary points of the potential energy surface through a vibrational analysis. The calculated spin density at the Pd atom is 1.50 for the triplet and 0.0 for the singlet.

The calculated Pd−O distances are longer than those experimentally determined by EXAFS in the **PdMn** compound and by XRD in other compounds with oxygen six-coordinated Pd(II). The apparent discrepancy could be expected due to the negative charge of the molecule calculated in the gas phase. Nevertheless, the significantly shorter basal distances calculated for the singlet state as compared to those of the triplet state nicely reflects the different occupation of the d orbitals that is strongly σ antibonding toward four equatorial donor atoms. Another significant difference between the two geometries is found in the asymmetric C═O stretching vibrational frequencies of the oxalate anions, that is calculated at 1694 cm^{-1} for the triplet, but at 1742 cm^{-1} for the singlet state. The former is definitely closer to the experimental values of 1698 and 1674 cm^{-1} found for **Pd2** and of 1699 and 1670 cm^{-1} found for Pd-linked oxalates in **PdMn**.

Calculations for the analogous tris(oxalato)nickelate(II) and tris(oxalato)platinate(II) anions show how diverse are the group 10 metal ions. While for Ni(II) the triplet in the octahedral geometry is more stable than the square-planar structure of the singlet by some 146 kJ mol^{-1}, for Pt(II) it is the other way around: the singlet is more stable by 67 kJ mol^{-1}. For Pd(II), both isomers differ by 8.3 kJ mol^{-1} for Pd(II) with the octahedral triplet as the most stable. These theoretical results nicely reflect the synthetic results on 3D oxalate-based networks. The environment around Ni(II) in $[Ru^{II}(bpy)_3][Ni^{II}_2(ox)_3]$ appears as a slightly trigonally distorted octahedron,[7] while it is impossible to insert the Pt(II) in the (10,3) anionic network where it would have been in a 6-fold environment. Experimentally and theoretically, Pd(II) confirms its borderline status: the compressed octahedral environment around the Pd(II) ion imposed in **Pd2** and **PdMn** by the topology of the anionic helices wrapped around the template tris(bipyridine)ruthenium(II) cation favors the triplet GS as compared to the singlet one. In contrast, when tris(bipyridine)ruthenium(II) cation fails to play its templating role, Pd(II) ends up in a square-planar singlet GS (Figure 1).

Although six-coordinate Pd(II) is much less common than the corresponding Ni(II) derivatives, such a situation is not unprecedented, as summarized in Table 2. It seems clear that the singlet state characteristic of square-planar Pd(II) complexes appears in six-coordinate complexes only when a significant tetragonal distortion is present, as illustrated by octahedral shape measures $S(O_h)$ (which indicates quantitatively the deviation from a perfectly octahedral geometry) exceeding 3 units.[54] Even if in our optimized tris(oxalato)palladate(II) anion, the corresponding shape measured for the triplet is 2.49, it reflects mostly the deviation from ideal octahedral angles induced by the small chelate angles of the oxalate ligand. In contrast, an octahedral measure of 6.67 is found for the optimized singlet state. As

(54) Stephenson, N. C. *J. Inorg. Nucl. Chem.* **1962**, *24*, 797.
(55) Alvarez, S.; Alemany, P.; Casanova, D.; Cirera, J.; Llunell, M.; Avnir, D. *Coord. Chem. Rev.* **2005**, *249*, 1693.

expected, the experimental data collected in Table 2 clearly indicate that the octahedral high spin situation is favorable for Pd(II) in the presence of the most electronegative π-donor atoms such as F or O, whereas donor sets that incorporate less electronegative atoms, such as Cl, N, S, I, P, or As, favor the tetragonally distorted (nearly square-planar) singlet state.

For a tetranuclear model of the PdMn network, $[Pd^{II}\{(\mu\text{-ox})\text{-}Mn^{II}(OH_2)_4\}_3]^{2+}$, we have also calculated the energy difference between the ferro- and antiferromagnetically coupled states, corresponding to total spins of $^{17}/_2$ and $^{13}/_2$, respectively. The antiferromagnetic state is found to be more stable by 404 cm^{-1}, corresponding to an exchange coupling constant $J = -19.2$ cm^{-1}.

Concluding Remarks

A 6-fold oxygenated environment has been generated around palladium(II) ions. It results from the strong template effect of tris(2,2′-bipyridine)ruthenium(II) in the synthesis of three-dimensional (3D) 10-gon 3-connected (10,3) oxalate-based networks. The structural characterization of $[Ru^{II}(bpy)_3][Mn^{II}\text{-}Pd^{II}(ox)_3]$ is based on the complementary analysis of X-ray powder diffraction and X-ray absorption spectroscopy data. It leads to the conclusion that the palladium(II) exhibits a compressed octahedral environment while manganese(II) has the "standard" trigonally distorted octahedral environment. Thanks to the 6-fold environment, palladium(II) has a triplet ($S = 1$) ground state. It couples antiferromagnetically with its manganese(II) neighbors. Both the structural and the magnetic results are supported by a computational study, which underlines the experimental borderline behavior of palladium(II) among group 10 metal ions between an octahedral triplet ground state and a (nearly) square-planar singlet one.

Acknowledgment. We thank CNRS (France), Université Pierre et Marie Curie-Paris 6 (France), and DFG (SPP 1137) for financial support. This research has also been supported by the Dirección General de Investigación del Ministerio de Educación y Ciencia and Comissió Interdepartamental de Ciència i Tecnologia (CIRIT) through grants CTQ2005-08123-C02-02/BQU and 2005SGR-00036, respectively. The computing resources used were generously made available at the Centre de Computació de Catalunya (CESCA) through a grant provided by Fundació Catalana per a la Recerca (FCR) and the Universitat de Barcelona. The stay of M.V. in Barcelona as Visiting Professor, which made this collaboration possible, was supported by ICREA.

Supporting Information Available: Crystallographic data (excluding structure factors) for the structure of $[Ru^{II}(bpy)_3][Pd^{II}_2Cl_6]\cdot{}^1/_2H_2O$ and $[Ru^{II}(bpy)_3]_2[Pd^{II}(ox)_2][Pd^{II}Cl_4]\cdot 11H_2O$ have been deposited at the Cambridge Crystallographic Data Centre with CCDC numbers 621724 and 621725, respectively. These data can be obtained free of charge from the Cambridge Crystallographic Data Centre via www.ccdc.cam.ac.uk/datarequest/cif. Also included are CIF files of the structures as well as the details on the EXAFS analysis. This material is available free of charge via the Internet at http://pubs.acs.org.

JA066817V